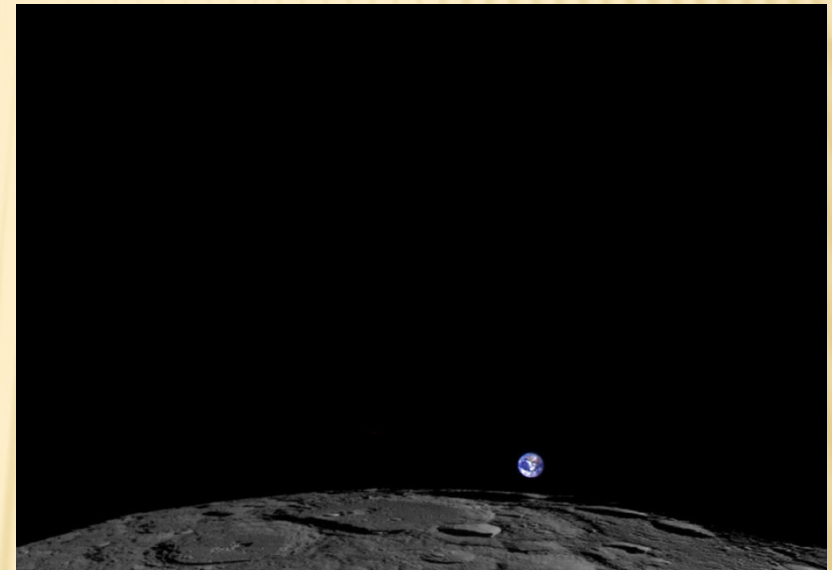

FORMATION OF WEAK MAGNETIC PROPERTIES IN LUNAR DUSTY PLASMA

**Prof. E.V. Martysh,
Taras Shevchenko National University, Kyiv, Ukraine**

LUNAR SURFACE

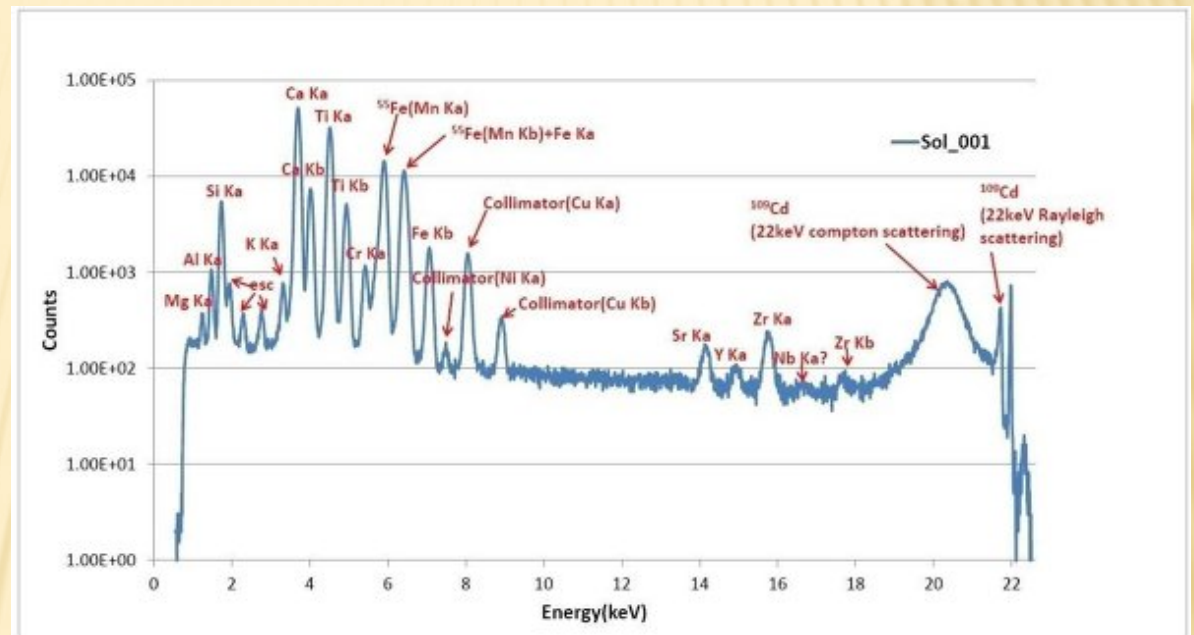


APOLLO Mission



The Lunar Reconnaissance
Orbiter, Earthrise From
Moon Feb. 1, 2014

LUNAR SOIL COMPOSITION



X-ray fluorescence spectrum of lunar regolith, the resulting device APXS on board the Chinese lunar rover "Jade Rabbit"

THE CHEMICAL AND ELEMENTAL COMPOSITION

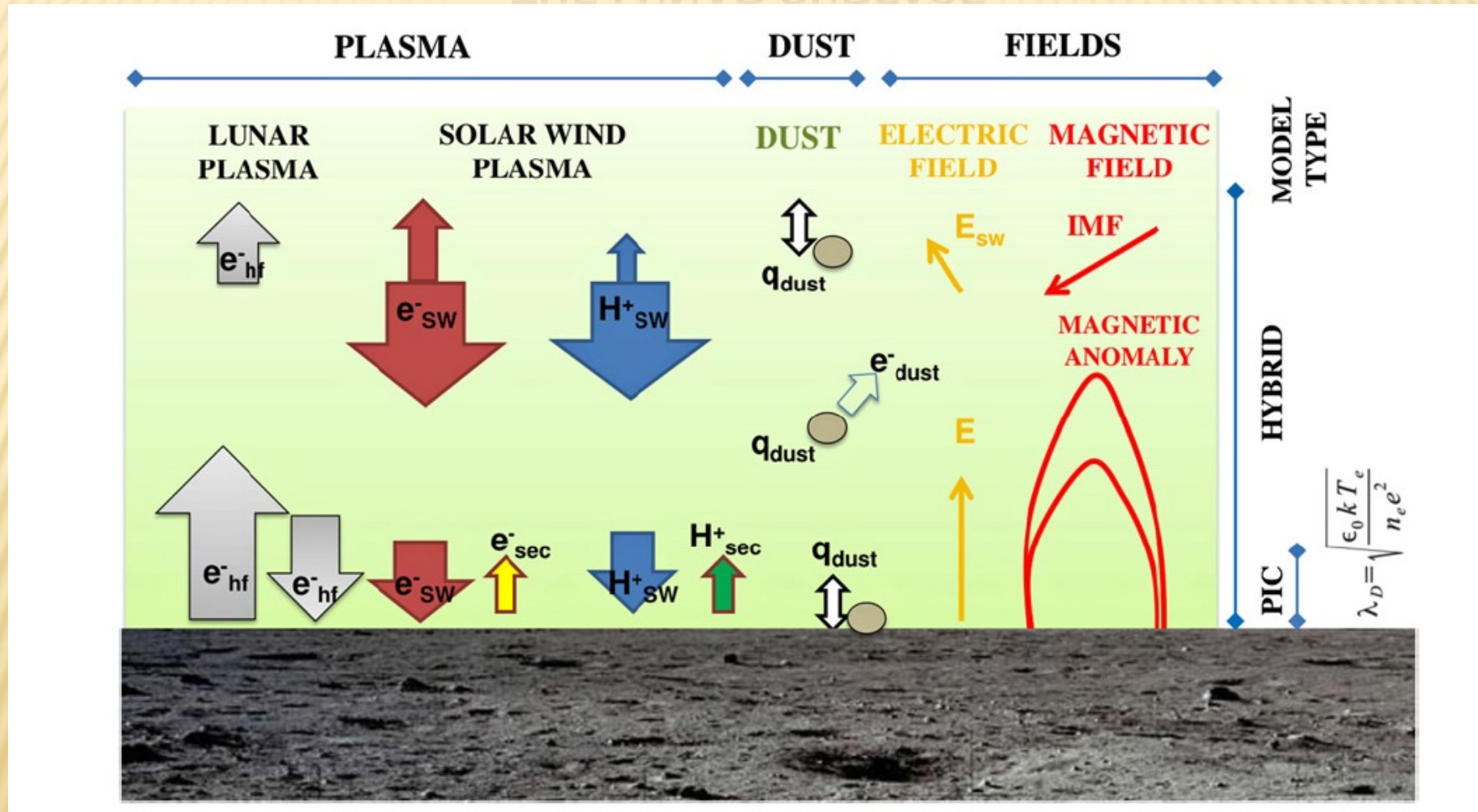
The elemental composition of lunar regolith (in%)

Element	Basalt	Mainland regolith	Regolith individual basins
Ca	7,9	10,7	7,7
Mg	5,8	4,6	6,1
Fe	13,2	4,9	3,7
Al	6,8	13,3	9,8
Ti	3,1	-	-
Si	20,4	21,0	21,8
O	41,3	44,6	43,3
S	0,1	0,072	0,076
K	0,1	0,073	0,24
Na	0,3	0,48	0,38

The chemical composition of the sea regolith (basalt) and mainland regolith (in %)

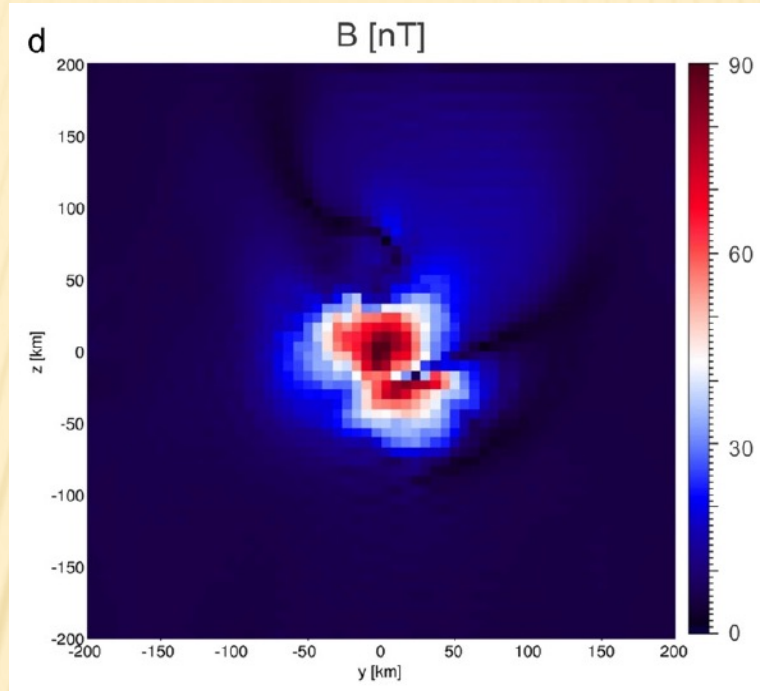
Composition	Basalt	Mainland regolith
SiO ₂	41,7	44,4
Al ₂ O ₃	15,33	22,9
TiO ₂	3,39	0,56
FeO	16,64	7,03
MgO	8,78	9,7
CaO	12,49	15,2
Na ₂ O	0,34	0,55
K ₂ O	0,1	0,1
MnO	0,21	0,12
Cr ₂ O ₃	0,28	-
P ₂ O ₅	0,12	0,14

A SCHEMATIC ILLUSTRATION OF PLASMAS AND FIELDS WHICH AFFECT THE LUNAR PLASMA ENVIRONMENT NEAR THE LUNAR SURFACE:



Esa Kallio, e.a., Kinetic simulations of finite gyroradius effects in the lunar plasma environment on global, meso, and microscales, Planetary and Space Science 74, 146–155, 2012.

THE LUNAR MAGNETIC ANOMALIES IN THE PIC MODEL



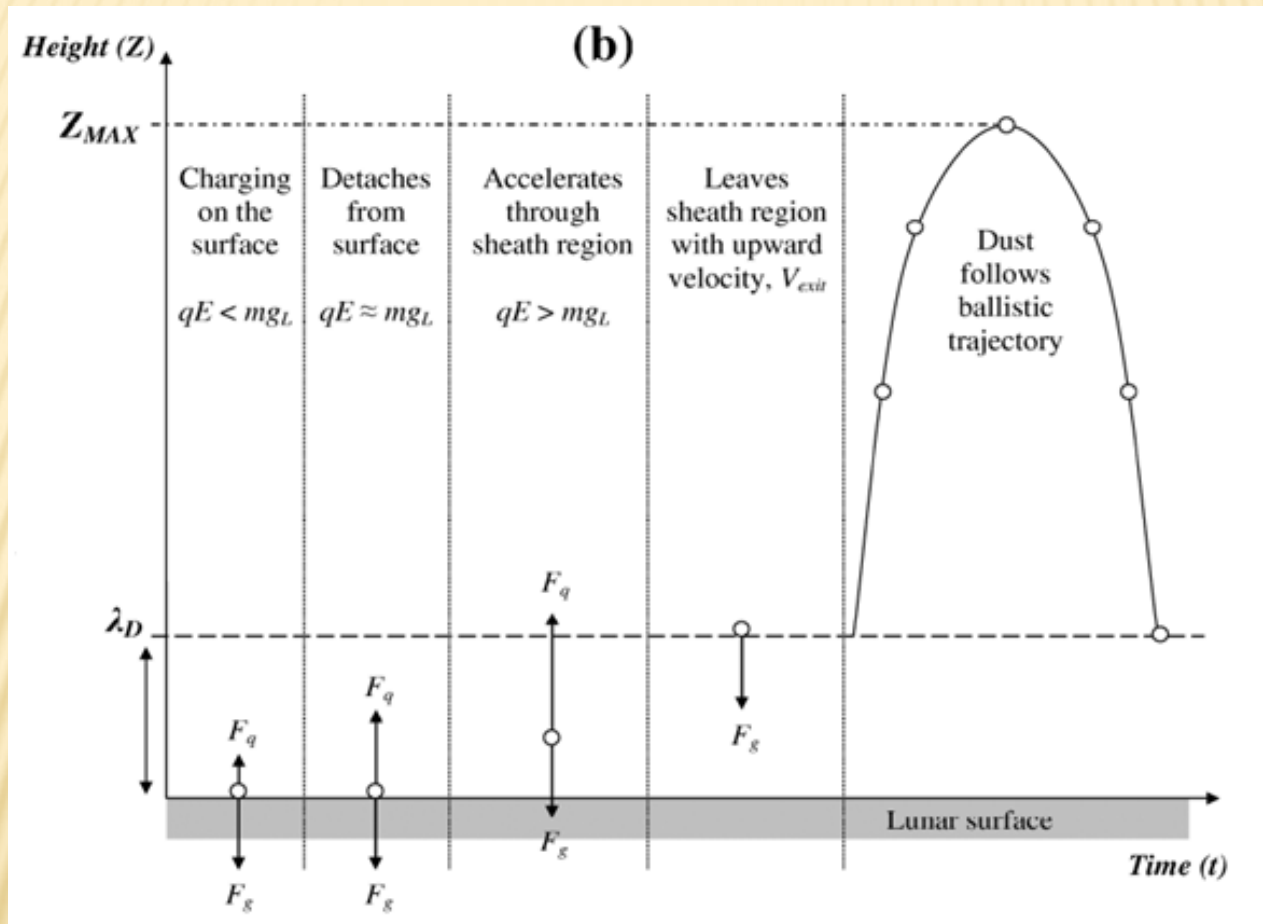
The lunar magnetic anomalies were discovered by the Apollo 12 magnetometer deployed on the lunar surface and by Explorer 35 from orbit [1].

The surface fields measured by Apollo 12, 14, 15, and 16 magnetometers were 38, 103, 3, and 327 nT, respectively [1].

Satellite observations showed that the largest and strongest magnetic fields, responsible for most of the solar wind limb disturbances were located on the lunar far side [2].

LP/ER measurements (Lunar Prospector electron reflectometry) suggests that the surface magnetic field strengths could reach thousands of nanotesla in some locations [3].

DYNAMIC FOUNTAIN MODEL



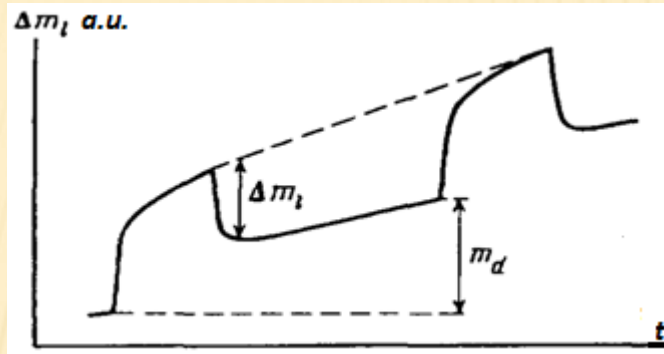
The evolution of a dust grain in dynamic fountain model

T. J. Stubbs, R. R. Vondrak and W. M. Farrell A DYNAMIC FOUNTAIN MODEL FOR LUNAR DUST. Lunar and Planetary Science XXXVI (2005)

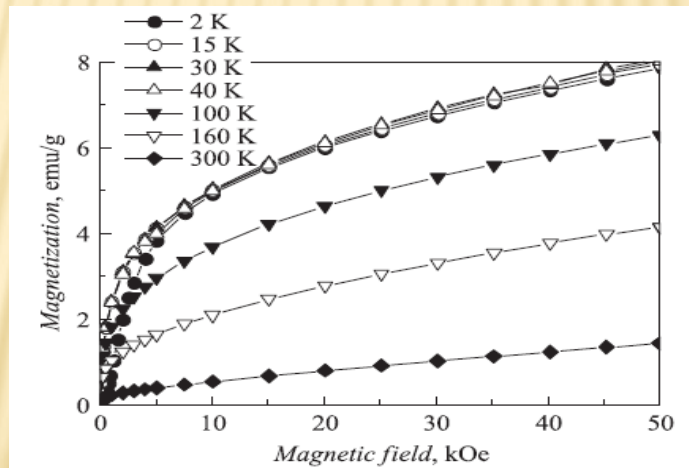
PARAMETERS OF THE NEAR-SURFACE PLASMA ENVIRONMENT FOR DIFFERENT SOLAR ACTIVITY CONDITIONS

	Equation	Solar Min.	Solar Max.	Solar Flare
Photoelectron current density J_{ph} ($\mu\text{A}/\text{m}^2$)	$J_{ph} = q \int_W^\infty Y(E) S(\lambda) \frac{d\lambda}{dE} dE.$	5.05	15.5	40
Surface potential ϕ_L (V)	$J_{ph} = J_{SW}$	5.0	7.2	9.1
Plasma density n_e (cm^{-3})	$n_e \cong 2 J_{ph,0} / \sqrt{T_{ph}/m_e},$	106	330	840
Debye length λ_D (cm)	$\lambda_D = \sqrt{\epsilon_0 T_{ph}/n_e q^2} ,$	100	60	36
Surface electric field E (V/m)	$E \cong \phi_L/\lambda_D$	4.9	12.5	25
Surface charge density $\sigma(10^{-10} \text{ C/m}^2)$	$\sigma = E \epsilon_0$	0.43	1.1	2.2
E^2 (V^2/m^2)	$[\phi_L/\lambda_D]^2$	23.7	153	632

IRRADIATION INFLUENCE ON MAGNETIC PROPERTIES

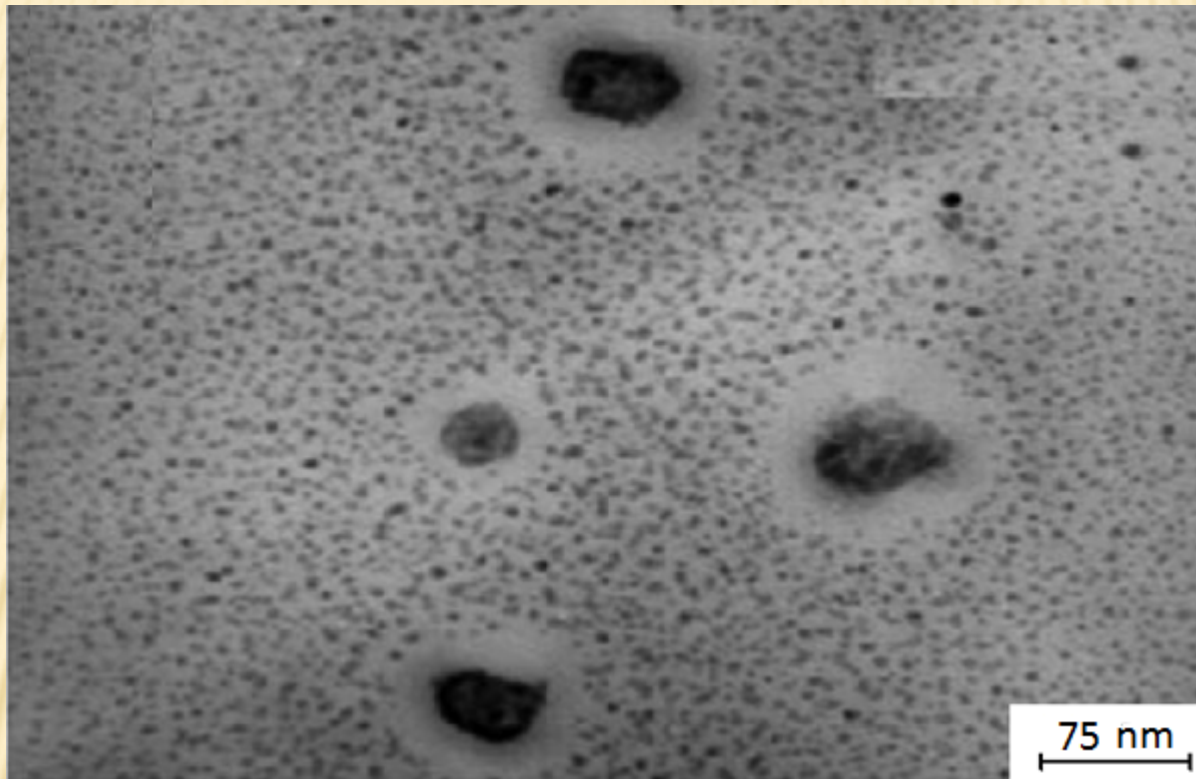


Temporary change of the magnetization: m_d - domain restructuring;
☒ m_t - photoinduced change in magnetization



Magnetization curves of nanocomposite with manganese-zinc ferrite particles $\text{Mn}_{0.5} \text{Zn}_{0.5} \text{Fe}_2\text{O}_4$, measured at different temperatures.

DIFFERENT WAYS OF METAL EVAPORATION FOR MAGNETIC NANOPARTICLES (CLUSTERS) PRODUCTION:



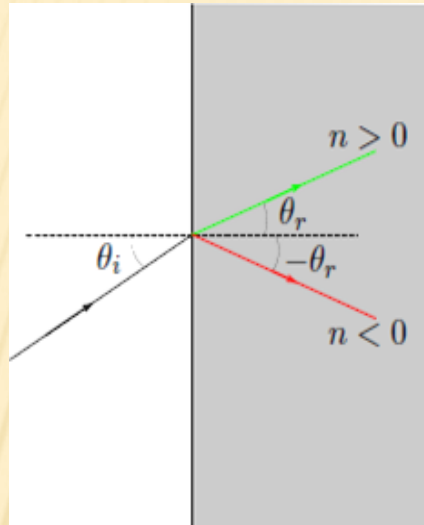
Photomicrograph of iron nanoparticles

Laser evaporation; thermal evaporation; arc, plasma evaporation; evaporation under the influence of solar energy. There is also a synthesis of the nanoparticles in a stream of hydrogen plasma (HPRM) and LECBD method (Low Energy Cluster Beam Deposition). The latter consists in depositing on the substrate uncharged particles with low kinetic energy.

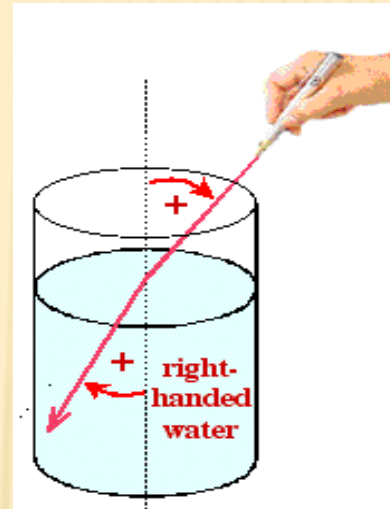
CHANGES IN THE MAGNETIC PROPERTIES

Object description	Characteristic dimension	Specific magnetic entities
Macroscopic sample	$\text{m} \text{ } 1 \text{ } \text{m}$	The spontaneous magnetization at $T \leq T_C$. Formation of the domains.
Microscopical sample	50 - 1000 nm	The magnetic characteristics depend strongly on the prehistory of the sample and its processing
Small magnetic particles in a diamagnetic matrix	1 -30 nm	The presence of the blocking temperature $T_b \leq T_C$. At temperatures $T > T_b$ particle proceeds to superparamagnetic state
Single atom	$\sim 0,2 \text{ nm}$	"Conventional" paramagnetic properties

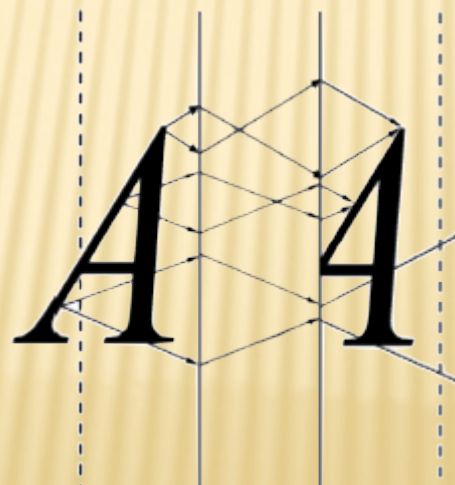
LEFT-HANDED MEDIA (LHM)



Ray diagram for an LH medium

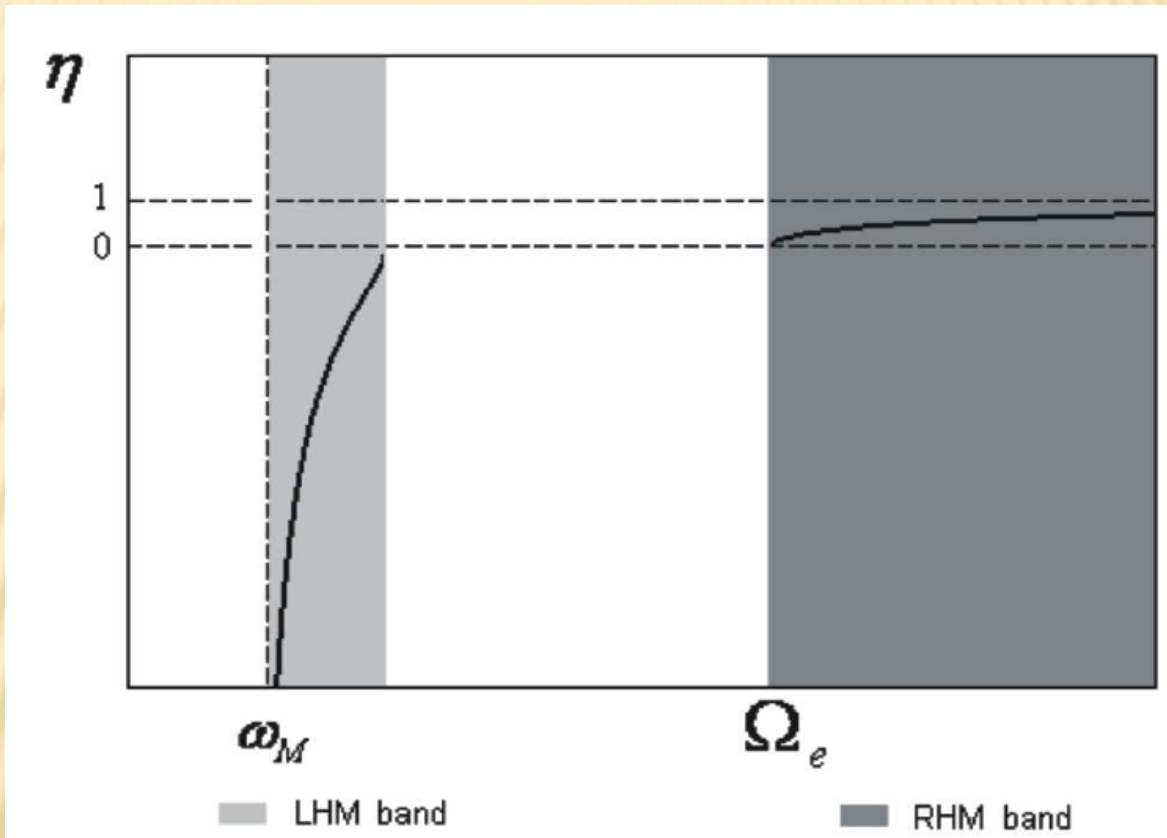


LHM representation



A three-dimensional image obtained by means of a plane-parallel plate made of a left-handed material.

LHM-PLASMA



Behavior of the LHM-Plasma refractive index

CONCLUSIONS

1. The magnetic properties of the lunar exosphere are determined by:
 - chemical composition of the microparticles in the lunar dusty plasma;
 - the intensity of the sunlight within a certain range.
2. Map of the lunar magnetic anomalies is necessary for more in-depth study of these issues
3. Left-handed media can be formed from Dusty plasma with ferromagnetic grains